Original Article Exploration of the mechanism of Tongmai Jiangzhuo Decoction in treating atherosclerosis based on network pharmacology and experimental validation

Ying Xu^{1*}, Hua Shi^{2*}, Changqing Ma^{2*}, Youyang Zhao³, Zhiqin Niu², Xinrui Gao², Yun Zhang⁴, Xiang Li^{2,5}, Yunpeng Luan², Jie Xia⁴, Guihui Wang⁶

¹First Clinical Medical College, Yunnan University of Chinese Medicine, Kunming 650500, Yunnan, China; ²Yunnan University of Chinese Medicine, Kunming 650500, Yunnan, China; ³Faculty of Biological and Food Engineering, Southwest Forestry University, Kunming 650224, Yunnan, China; ⁴The First Affiliated Hospital of Yunnan University of Chinese Medicine, Kunming 650021, Yunnan, China; ⁵Yunnan Provincial Clinical Medical Center for Chinese Medicine (Spleen and Stomach Diseases), Kunming 650021, Yunnan, China; ⁶The Third Affiliated Hospital of Yunnan University of Chinese Medicine, Kunming 650000, Yunnan, China. *Equal contributors and co-first authors.

Received June 14, 2025; Accepted August 10, 2025; Epub September 15, 2025; Published September 30, 2025

Abstract: Objectives: Atherosclerosis (AS) is a dyslipidemia-driven immunoinflammatory disease. While Tongmai Jiangzhuo Decoction (TMJZ) clinically improves cardiovascular outcomes through lipid-lowering effects, its molecular mechanisms against AS remain unelucidated. This study aimed to systematically investigate the anti-atherogenic mechanisms of TMJZ. Methods: Main active components of TMJZ and their targets were identified using Traditional Chinese Medicine Systems Pharmacology Database (TCMSP) and Bioinformatics Analysis Tool for Molecular mechANism of TCM (BATMAN-TCM). Potential therapeutic targets were sourced from Online Mendelian Inheritance in Man (OMIM) and GeneCards. Protein-protein interactions (PPI) network, Gene Ontology (GO), and Kyoto Encyclopedia of Genes and Genomes (KEGG) analyses were conducted using Cytoscape. Molecular docking was performed with AutoDockTools, AutoDock Vina, and PyMOL. Apolipoprotein E (ApoE)-deficient mice were used to validate the targets. Results: A total of 395 predicted intersection target genes between TMJZ targets and atherogenic-related targets were identified. Key anti-atherosclerosis targets of TMJZ included Peroxisome Proliferator-Activated Receptor Gamma (PPARy), Cluster of Differentiation 36 (CD36, fatty acid translocase), Interleukin 6 (IL6), Insulin (INS), AKT Serine/Threonine Kinase 1 (AKT1), Tumor Necrosis Factor (TNF), Tumor Protein p53 (TP53), Interleukin 1 Beta (IL1B), Catenin Beta 1 (CTNNB1), and Apolipoprotein E (APOE). Among these, PPARy/CD36 signaling emerged as a pivotal pathway. In vivo studies demonstrated that TMJZ improved blood lipids, reduced plaque area and lipid deposition, upregulated PPARy expression, and downregulated CD36 expression in aortic tissues. Additionally, TMJZ upregulated Liver X Receptor Alpha (LXRα) and ATP Binding Cassette Subfamily A Member 1 (ABCA1), promoting reverse cholesterol transport. Conclusions: TMJZ alleviates atherosclerosis by inhibiting lipid uptake via the PPARy/ CD36 pathway.

Keywords: Atherosclerosis, TMJZ, network pharmacology, CD36, PPARy

Introduction

Atherosclerosis (AS), characterized by the thickening and hardening of large- or medium-sized arteries, is a leading cause of plaque formation, stenosis, rupture, and bleeding. As the major cause of death and disability worldwide, cardiovascular and cerebrovascular diseases present a critical global health challenge [1]. In

2015 alone, cardiovascular diseases (CVDs) affected approximately 422.7 million individuals and resulted in over 17 million deaths. Alarmingly, the affected population is becoming progressively younger, posing a substantial threat to human health and life [2, 3]. While current treatments such as statins and surgery offer some benefit against AS, they are associated with inevitable sequelae [4-6]. Con-

sequently, investigating the underlying mechanisms of AS and discovering novel therapeutic agents remains highly important.

Tongmai Jiangzhuo Pill (TMJZ) is a promising traditional Chinese medicine (TCM) formulation. Developed through long term clinical practice by experts at the First Affiliated Hospital of Yunnan University of Chinese Medicine, this pure herbal preparation contains Panax notoginseng, Salvia miltiorrhiza, Hawthorn, Rhizoma alismatis, Astragalus membranaceus, Ganoderma lucidum, Polygonum multigonum, Angelica sinensis, Ligusticum chuangxiong, Red peony, Leonurus leonurus, Leech, and other components. The formula functions to activate blood circulation, resolve stasis, and eliminate turbidity. It is particularly effective for coronary atherosclerosis presenting with qi stagnation, blood stasis, and phlegm turbidity, demonstrating widespread clinical use and remarkable efficacy. Previous studies confirm that TMJZ effectively reduces serum total cholesterol (TC) and triglyceride (TG) levels in AS patients, regulates lipid metabolism disorders, improves plaque properties, and may inhibit coronary atherosclerosis formation by modulating platelet adhesion and activation function [7, 8]. However, the precise molecular mechanisms by which TMJZ exerts its therapeutic effects on AS remain poorly understood.

Network pharmacology, integrating pharmacology, informatics, systems biology, and computer science [9, 10], provides a powerful approach for analyzing the mechanisms of multi-target drugs and identifying pharmacodynamic substances within TCM. Molecular docking further complements this by predicting the binding modes and binding free energies between proteins and ligands, offering validation for predicted pharmacological functions and mechanisms. Therefore, this study employed an integrated approach combining network pharmacology and molecular docking to elucidate the potential mechanisms of TMJZ in treating AS. We investigated the anti-AS effects of TMJZ in atherosclerotic ApoE deficient mice and subsequently evaluated the predictive ability of the network pharmacology approach. Finally, the key targets identified computationally were experimentally validated (Figure 1).

Materials and methods

Potential targets identification of TMJZ and atherosclerosis

The compounds of TMJZ and their corresponding targets were obtained from Traditional Chinese Medicine Systems Pharmacology Database (TCMSP) (https://old.tcmsp-e.com/ tcmsp.php) [9] and Bioinformatics Analysis Tool for Molecular mechANism of TCM (BAT-MAN-TCM)(http://bionet.ncpsb.org.cn/batmantcm/index.php) [10]. Filters applied included OB (Oral Bioavailability) ≥ 30% and DL (Drug-Likeness) ≥ 0.18. AS-related genes were screened from the Online Mendelian Inheritance in Man (OMIM) (https://omim.org/) and Gene-Cards, using the keyword "atherosclerosis", with the targets in this study limited to human genes. Disease and drug targets were standardized as Gene Symbols using Uniprot database. Venn diagrams, generated using Venny 2.1 software, were used to visualize the intersection between drug and disease targets.

Construction of component-target-disease (CTD) and protein-protein interaction (PPI) networks

The intersection targets of the TMJZ and AS were imported into Cytoscape 3.8.2 to construct the CTD network. The species was set to Homo sapiens, and the minimum required interaction score was 0.90. Protein-protein interaction (PPI) was constructed via STRING (https://cn.string-db.org/) and then visualized with Cytoscape 3.8.2 software to identify potential core target networks. Betweenness centrality (BC), closeness centrality (CC), and degree centrality (DC) were calculated via CytoNCA for core target identification.

GO and KEGG enrichment analysis of TMJZ components and AS targets

DAVID (https://david.ncifcrf.gov/) [11] was used to collect data for Gene Ontology (GO) analysis of biological processes (BP), cellular components (CC) and molecular functions (MF) [12], as well as for Kyoto Encyclopedia of Genes and Genomes (KEGG) enrichment analysis. These analyses were then further evaluated by Bioinformatics (http://www.bioinformatics.com.cn/).

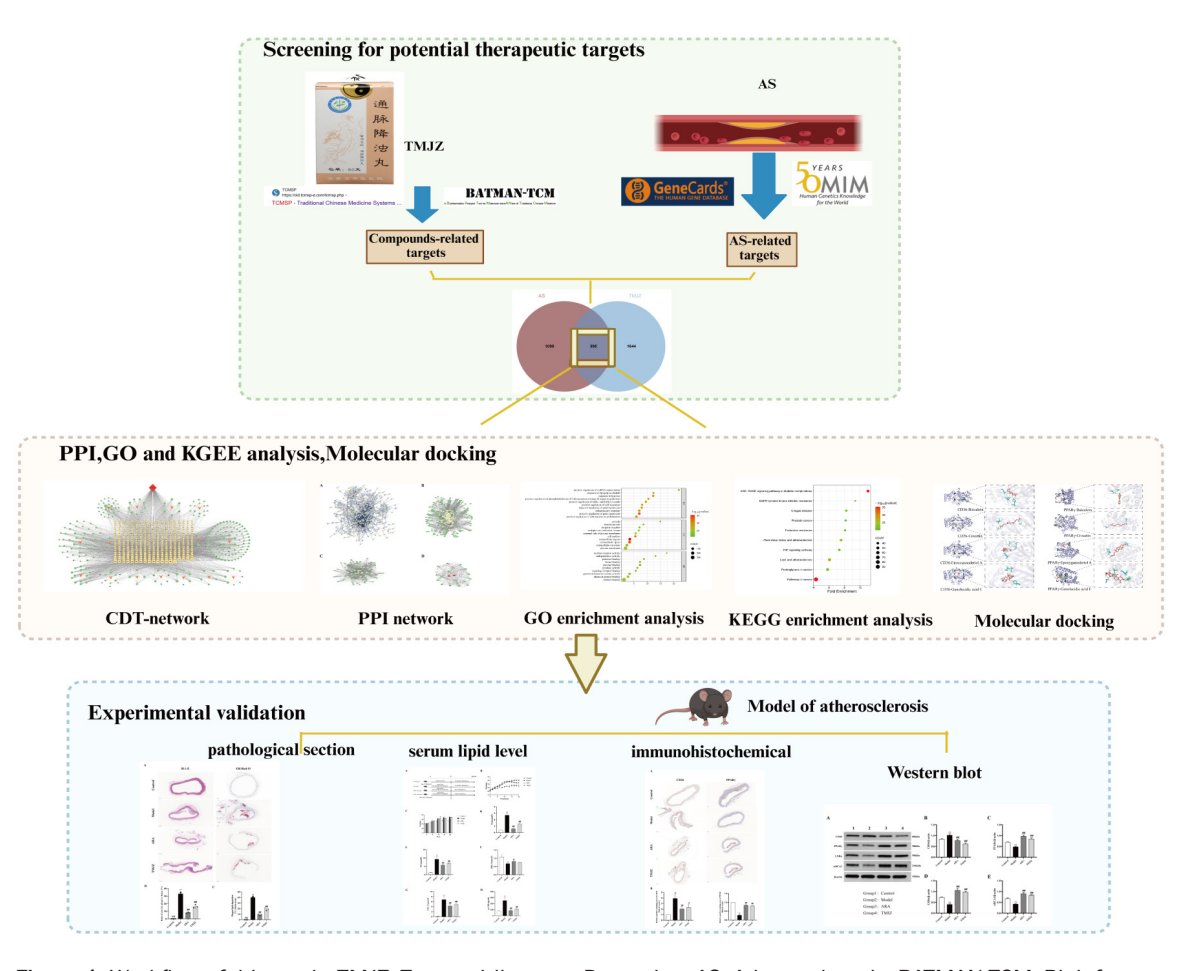


Figure 1. Workflow of this study. TMJZ, Tongmai Jiangzuo Decoction; AS, Atherosclerosis; BATMAN-TCM, Bioinformatics Analysis Tool for Molecular mechANism of Traditional Chinese Medicine; OMIM, Online Mendelian Inheritance in Man; PPI, Protein-Protein Interaction; GO, Gene Ontology; KEGG, Kyoto Encyclopedia of Genes and Genomes; CDT, Cluster and Data Triangulation.

Molecular docking validation

Molecular docking of core components and targets was performed. The 3D crystal structures of targets were retrieved from Protein Data Bank (PDB) at https://www.rcsb.org/. The pdb-format files were downloaded, dehydrated, hydrogenated, and prepared as receptors using AutoDockTools (version 1.5.7) (https://ccsb.scripps.edu/mgltools/downloads/), then saved as pdbqt files. The sdf files of the components were obtained from the PubChem database, hydrogenated using AutoDockTools, selected as ligands, and exported as pdbqt files. Molecular docking was performed with AutoDock Vina, and results were visualized by PyMOL.

Preparation of TMJZ

TMJZ is composed of Panax notoginseng, Salvia miltiorrhiza, Crataegus pinnatifida, Astr-

agalus membranaceus, Ganoderma lucidum, Polygonum multiflorum, Lycium barbarum, Angelica sinensis, Ligusticum chuanxiong, Paeonia lactiflora, Leonurus japonicus, Hirudo, Alisma orientale, Cassia obtusifolia, and Nelumbo nucifera leaf. The pill formulation (specification: 22 pills \approx 1 g, equivalent to 1.16 g crude herbs per 1 g preparation) was vacuum-dried and pulverized into a fine powder. For administration, the powder was suspended in physiological saline to prepare a solution at 0.26 g/mL (calculated based on the preparation weight). This concentration was derived from the human clinical dose (10 g, twice daily) converted to a murine equivalent (2.6 g/ kg/day) using body surface area normalization [13], accounting for a maximum tolerable gavage volume of 0.1 mL/10 g body weight in mice. The suspension was vortexed and sonicated to ensure homogeneity before use.

Animal study

Male apolipoprotein E knockout (ApoE-/-) mice and C57BL/6J mice (6 weeks old, 21-24 g) were obtained from Zhishan (Beijing) Health Medical Research Institute Co., LTD. (SCXK (Beijing) 2022-0009) and housed in a Specific Pathogen-Free (SPF) laboratory. All animal experiments were conducted in strict accordance with protocols approved by our institutional Animal Ethics Committee (approval number R-0620-21ZH-036). After a week of acclimatization, ApoE-/- or C57BL/6J mice were fed a high-fat diet (HFD: 78.85% basal diet, 21.00% fat, and 0.15% cholesterol) or standard chow diet for 24 weeks. Three mice from each group were randomly chosen and sacrificed after 12 weeks for Hematoxylin and Eosin (H&E) staining and serum lipid level analysis to assess AS degree [14]. ApoE-/- mice were separated into 3 groups: model (normal saline 10 mL/kg/day, i.g.), Atorvastatin group (ARA, 1.5 mg/kg/day, i.g.), and TMJZ group (2.6 g/kg/day, i.g.). At the end, mice were fasted for 12 h before execution for sampling. The atorvastatin dose (1.5 mg/kg/ day) was derived from the standard human dose (20 mg/day) using the same conversion method, consistent with established protocols for murine atherosclerosis studies (Figure 7A) [13].

All animal procedures were conducted in accordance with ethical guidelines for animal welfare. Before surgical procedures, mice were anesthetized using a small animal anesthesia machine (R500, RWD) with 3% isoflurane inhalation until loss of righting reflex. To minimize stress and suffering, animals were: (1) moved to a quiet room away from cage mates to prevent fear pheromone transmission; (2) habituated to gentle handling for 3-7 days prior to experiments; and (3) maintained at appropriate temperature (26°C) using heating pads to reduce cold-induced pain sensitivity. For euthanasia, animals were placed on a 37°C heating pad and initially anesthetized with 3% isoflurane at 1 L/min for 30-60 seconds until loss of righting reflex, then maintained at 1.5-2% isoflurane with 0.4-0.6 L/min flow rate via facemask. Throughout the procedures, respiratory rate, toe pinch, and corneal reflexes were monitored, with anesthesia adjusted as necessary. Following blood collection, animals were euthanized by maintaining 3-5% isoflurane for 1-2 minutes until cessation of heartbeat and respiration. Death was confirmed by observation of cardiac arrest, pupillary dilation, and absence of respiration.

Cytokines and plasma lipid analysis

Blood samples were collected from anesthetized mice via cardiac puncture and centrifuged at 1500 × g for 10 min at 4°C to isolate serum. Lipid profiles, including total cholesterol (TC), triglycerides (TG), high-density lipoprotein cholesterol (HDL-C), and low-density lipoprotein cholesterol (LDL-C), were quantified using commercial kits (Nanjing Jiancheng Bioengineering Institute, China; Cat# A110-1-1, A111-1-1, A112-1-1, A113-1-1) according to manufacturer protocols. Absorbance was measured at 500 nm (TC/TG) or 546 nm (HDL-C/LDL-C) using a microplate reader (BioTek Synergy H1, USA).

Serum oxidized LDL (ox-LDL) levels were determined with an ELISA kit (Wuhan Huamei Biotech, China; Cat# CSB-E07933m). Inflammatory cytokines (TNF- α , IL-1 β , IL-6) were analyzed using ELISA kits (Jiangsu Enzyme Immuno Biotechnology, China; Cat# MM-0180R2, MM-0047R2, MM-0057R2). Briefly, 100 μ L of serum or standard was added to antibody-precoated wells and incubated at 37°C for 90 min, followed by biotin-conjugated detection antibody (60 min, 37°C) and streptavidin-HRP (30 min, 37°C). After TMB substrate development, reactions were stopped with 2M $\rm H_2SO_4$, and absorbance was read at 450 nm. All samples were run in duplicate.

Histologic analysis of aorta

After 48 h fixation in 4% paraformaldehyde (PFA), aortic arches were processed as follows: for H&E staining, tissues were dehydrated, paraffin-embedded, and sectioned. For Oil Red O staining, tissues were cryoprotected in 30% sucrose, embedded in OCT compound, and sectioned at 10 μm using a cryostat. Sections were stained with hematoxylin (G1004-500ML), eosin (G1001-500ML), or Oil Red O (Cat: Y07512, Hefei Bomei), and observed under a microscope.

Immunohistochemical (IHC) staining

Peroxisome Proliferator-Activated Receptor Gamma (PPARγ) and Cluster of Differentiation 36 (CD36) expression in aortic arches were

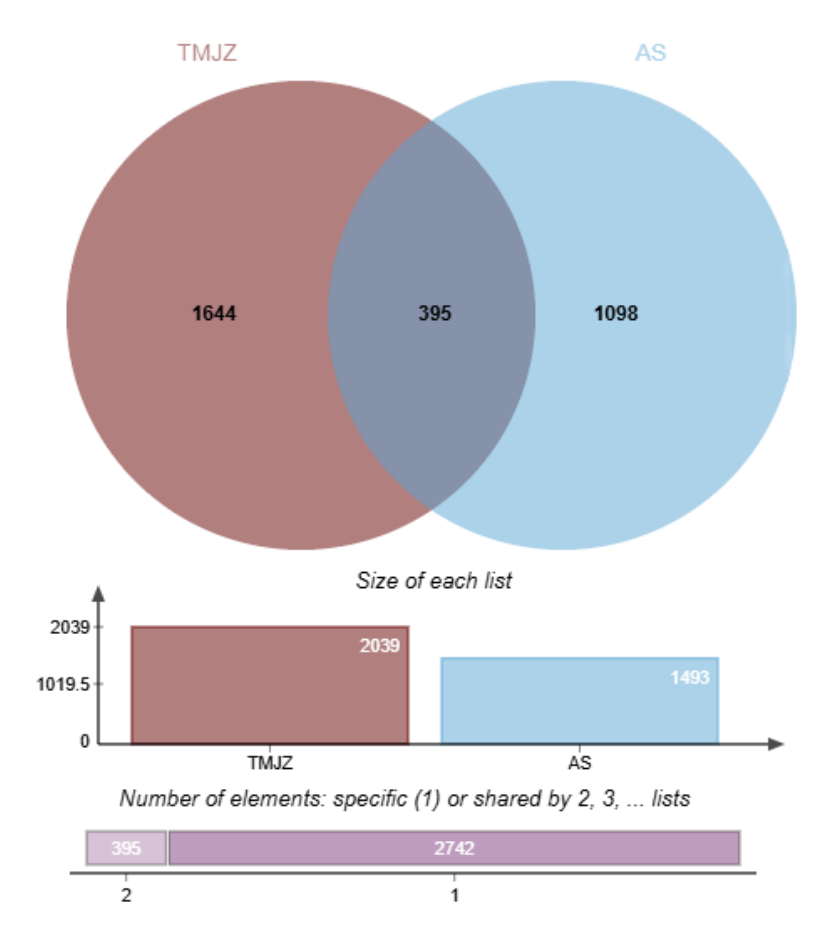


Figure 2. The intersection genes of AS-related and TMJZ-targeted genes displayed by Venn diagram. TMJZ, Tongmai Jiangzuo Decoction; AS, Atherosclerosis.

visualized by Immunohistochemistry (IHC). After dewaxing, rehydration, and blocking with 3% Bovine Serum Albumin (BSA), sections were incubated with PPARγ (Servicebio, 1:500) and CD36 (Servicebio, 1:600) antibodies at 4°C for 12 h, followed by incubation with secondary antibodies (Goat Anti-Rabbit Immunoglobulin G [IgG], Servicebio, 1:200) conjugated with HRP. After 3,3'-Diaminobenzidine (DAB) and hematoxylin staining, images were observed under a microscope.

Western blot

Western blot analysis was performed to evaluate the expression of CD36, PPARy, liver X receptor alpha (LXRa), and ATP-binding cassette transporter A1 (ABCA1) protein expression in mouse aorta samples. Proteins were extracted using radioimmunoprecipitation assay (RIPA) lysis buffer containing phenylmethylsulfonyl fluoride (PMSF), and the supernatant

was collected after centrifugation at 12,000 revolutions per minute (rpm) for 30 min at 4°C. Bicinchoninic acid (BCA) assay was used for protein quantification. After adding loading buffer and heating for denaturation, proteins were separated by sodium dodecyl sulfate-polyacrylamide gel electrophoresis (SDS-PAGE) and blotted to membranes, which were blocked by skim milk. Membranes were incubated overnight at 4°C with antibodies against CD36 (1:1000), PPARy (1:1000), LX-Rα (1:1000), ABCA1 (1:1000), and β -actin (1:2000). After washing, membranes were incubated with secondary (2nd) antibodies (1:1000). Bands were visualized using enhanced chemiluminescence (ECL).

Statistical analysis

Data were presented as mean ± standard deviation (SD) and analyzed using GraphPad Prism 8.3.0 software. For multiple group comparisons

(including serum lipids, cytokines, plaque area, and protein expression across Control/Model/ARA/TMJZ groups), one-way analysis of variance (ANOVA) with Tukey's post hoc test was applied for pairwise comparisons. Longitudinal body weight data were assessed by repeated-measures ANOVA with Greenhouse-Geisser correction, followed by Tukey's post hoc test. Normality was verified using the Shapiro-Wilk test, and homogeneity of variances was confirmed using Levene's test. Comparisons between two groups were performed using Student's unpaired t-test. A two-tailed *P*-value < 0.05 was considered significant for all analyses.

Results

Composition and target screening of TMJZ

Combined analysis of the TCMSP, BATMAN-TAM and Swiss Target Prediction databases identi-

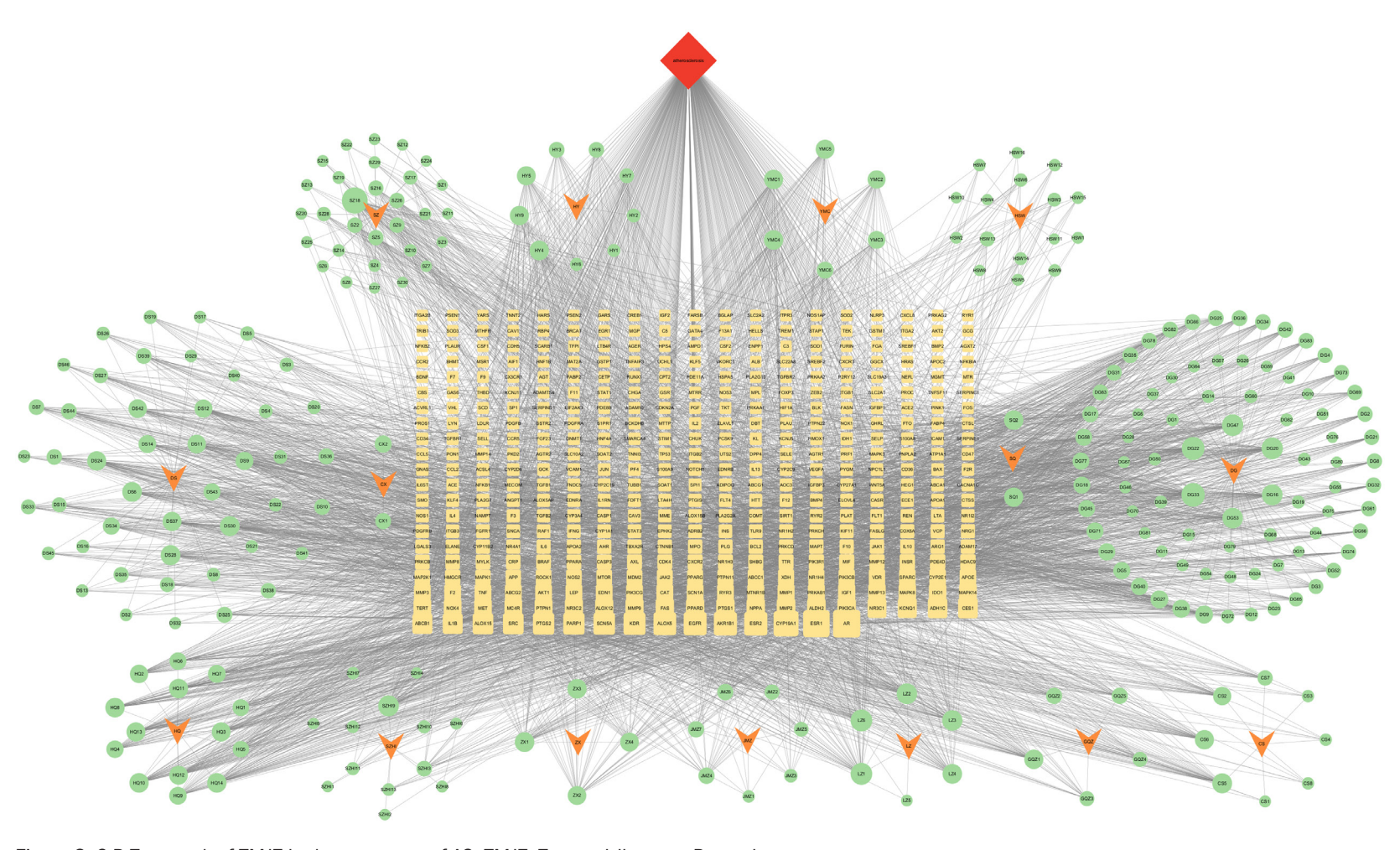


Figure 3. C-D-T network of TMJZ in the treatment of AS. TMJZ, Tongmai Jiangzuo Decoction.

Table 1. 20 bioactive compounds of TMJZ

MOL ID	Compound	OB (%)	DL	Botanical Drug	Pinyin	Degree
MOL001406	crocetin	35.30	0.26	Whitmania pigra	SHUIZHI	43.0
MOL011156	epoxyganoderiol A	33.78	0.83	Ganoderma	LINGZHI	41.0
MOL007123	miltirone II	44.95	0.24	Radix Salviae	DANGSHEN	39.0
MOL007120	miltionone II	71.03	0.44	Radix Salviae	DANGSHEN	39.0
MOL002714	baicalein	33.52	0.21	Radix Paeoniae Rubra	CHISHAO	39.0
MOL011256	ganolucidic acid E	32.85	0.82	Ganoderma	LINGZHI	38.0
M0L000832	alisol,b,23-acetate	32.52	0.82	Alisma Orientale (Sam.) Juz.	ZEXIE	38.0
MOL000354	isorhamnetin	49.6	0.31	Folium Nelumbinis	HEYE	37.0
M0L000853	alisol B	36.76	0.82	Alisma Orientale (Sam.) Juz.	ZEXIE	37.0
MOL000354	isorhamnetin	49.60	0.31	Leonuri Herba	YIMUCAO	37.0
MOL000417	Calycosin	47.75	0.24	Hedysarum Multijugum Maxim.	HUANGQI	37.0
MOL000098	quercetin	46.43	0.28	Panax Notoginseng	SANQI	36.0
MOL001002	ellagic acid	43.06	0.43	Radix Paeoniae Rubra	CHISHAO	36.0
MOL000006	luteolin	36.16	0.25	Radix Salviae	DANGSHEN	36.0
MOL000422	kaempferol	41.88	0.24	Hedysarum Multijugum Maxim.	HUANGQI	35.0
MOL001418	galeopsin	61.02	0.38	Leonuri Herba	YIMUCAO	31.0
MOL002157	wallichilide	42.31	0.71	Chuanxiong Rhizoma	CHUANXIONG	27.0
MOL001421	preleoheterin	85.97	0.33	Leonuri Herba	YIMUCAO	25.0
M0L002268	rhein	47.07	0.28	Cassiae Semen	JUEMINGZI	23.0
MOL006486	obtusin	31.24	0.40	Cassiae Semen	JUEMINGZI	23.0

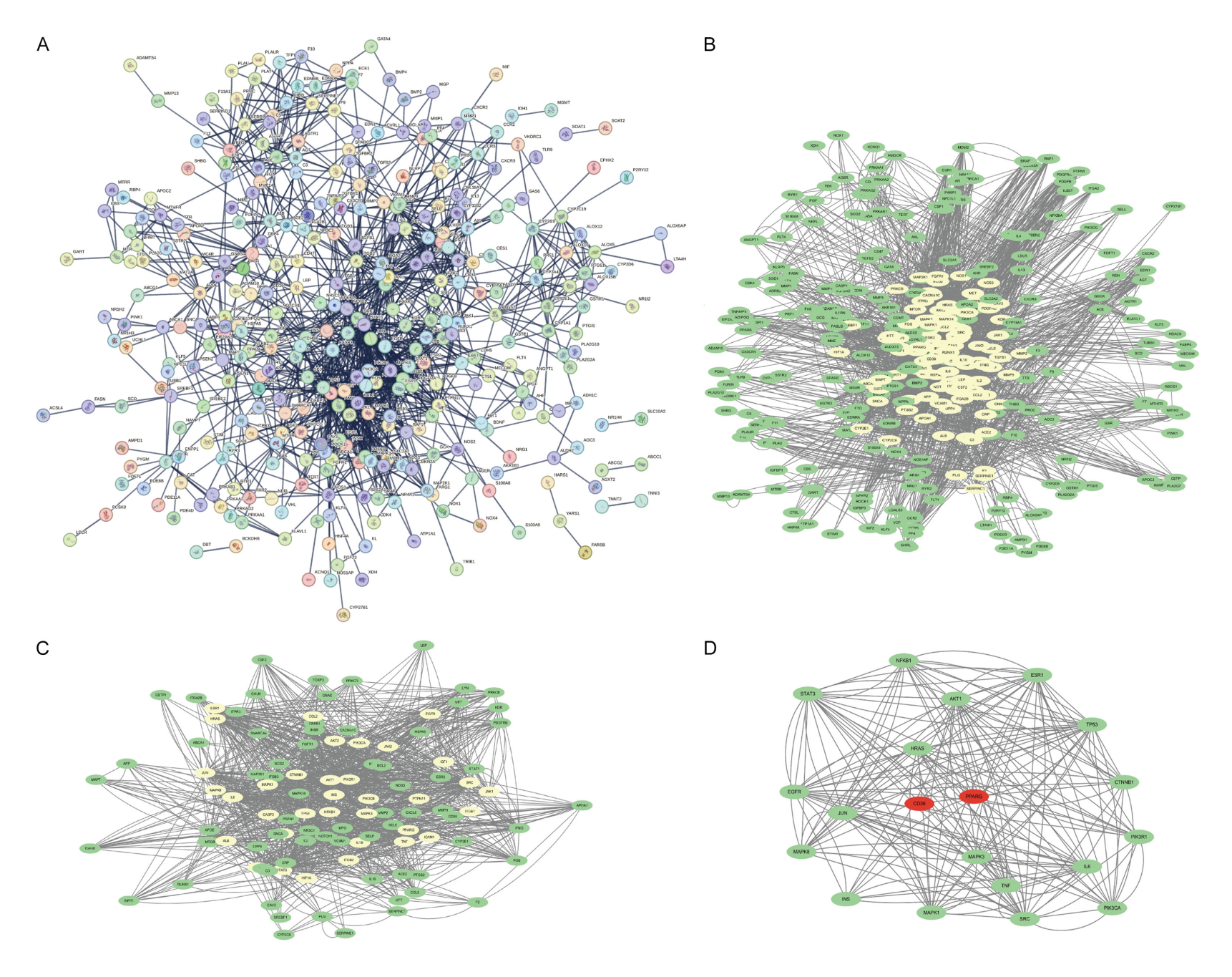
Table 2. Top 20 intersection targets

Target	Degree	Betweenness	Closeness	Target	Degree	Betweenness	Closeness
IL6	72	8984.947	0.39880952	CTNNB1	56	4673.2515	0.36853686
TNF	68	7760.227	0.39458185	MAPK1	62	2431.1462	0.36813188
STAT3	76	7294.082	0.39458185	MAPK8	38	2009.4146	0.36177105
SRC	86	8923.037	0.38550058	PIK3CA	58	1652.427	0.35867238
INS	52	11172.143	0.38505748	ESR1	52	2347.9539	0.35828876
AKT1	72	6159.9087	0.38417432	NFKB1	52	3305.404	0.3567625
TP53	86	9366.426	0.3811149	HRAS	50	2147.8352	0.35600424
JUN	62	4644.477	0.37767756	PIK3R1	54	1416.8796	0.35300317
MAPK3	64	3912.258	0.37305123	PPARG	34	4007.7576	0.35263157
EGFR	64	3649.929	0.37057522	CD36	34	2347.9327	0.39263157

IL6, interleukin-6; TNF, tumor necrosis factor; STAT3, signal transducer and activator of transcription 3; SRC, SRC protooncogene; INS, insulin; AKT1, AKT serine/threonine kinase 1; TP53, tumor protein p53; JUN, Jun proto-oncogene; MAPK3,
mitogen-activated protein kinase 3; EGFR, epidermal growth factor receptor; CTNNB1, catenin beta 1; MAPK1, mitogen-activated protein kinase 1; MAPK8, mitogen-activated protein kinase 8; PIK3CA, phosphatidylinositol-4,5-bisphosphate 3-kinase
catalytic subunit alpha; ESR1, estrogen receptor 1; NFKB1, nuclear factor kappa B subunit 1; HRAS, HRas proto-oncogene;
PIK3R1, phosphoinositide-3-kinase regulatory subunit 1; PPARG, peroxisome proliferator activated receptor gamma; CD36,
CD36 molecule.

fied: two active ingredients of *Panax notoginseng*, corresponding to 167 target genes; 46 active components of *Salvia miltiorrhiza*, corresponding to 688 target genes; 30 active components of *hawthorn*, corresponding to 555 target genes; 14 active components of *Astragalus membranaceus*, corresponding to 348

target genes; 6 active ingredients of *Ganoderma lucidum*, corresponding to 260 target genes; 16 active components of *Polygonum multiflorum*, corresponding to 203 target genes; 5 active components of *L. barbarum*, corresponding to 225 target genes; 83 active ingredients of *Angelica sinensis*, corresponding to



TMJZ inhibits atherosclerosis through PPARy/CD36

Figure 4. PPI network of TMJZ-AS. (A) The interactive PPI network obtained from STRING database with species limited to "Homo sapiens", the minimum required interaction score set to 0.90, and the independent target protein nodes hidden. (B) Original PPI network from STRING database imported to Cytoscape 3.8.2 to obtain a new network. It contains 336 nodes and 2642 edges. (C) PPI network screened from (B) in Cytoscape 3.8.2. It contains 106 nodes and 1210 edges. (D) Core PPI network screened from (C) in Cytoscape 3.8.2. It contains 20 nodes and 178 edges. Larger node sizes indicate higher degree values. TMJZ, Tongmai Jiangzuo Decoction; AS, Atherosclerosis; PPI, protein-protein interaction; STRING, Search Tool for the Retrieval of Interacting Genes/Proteins.

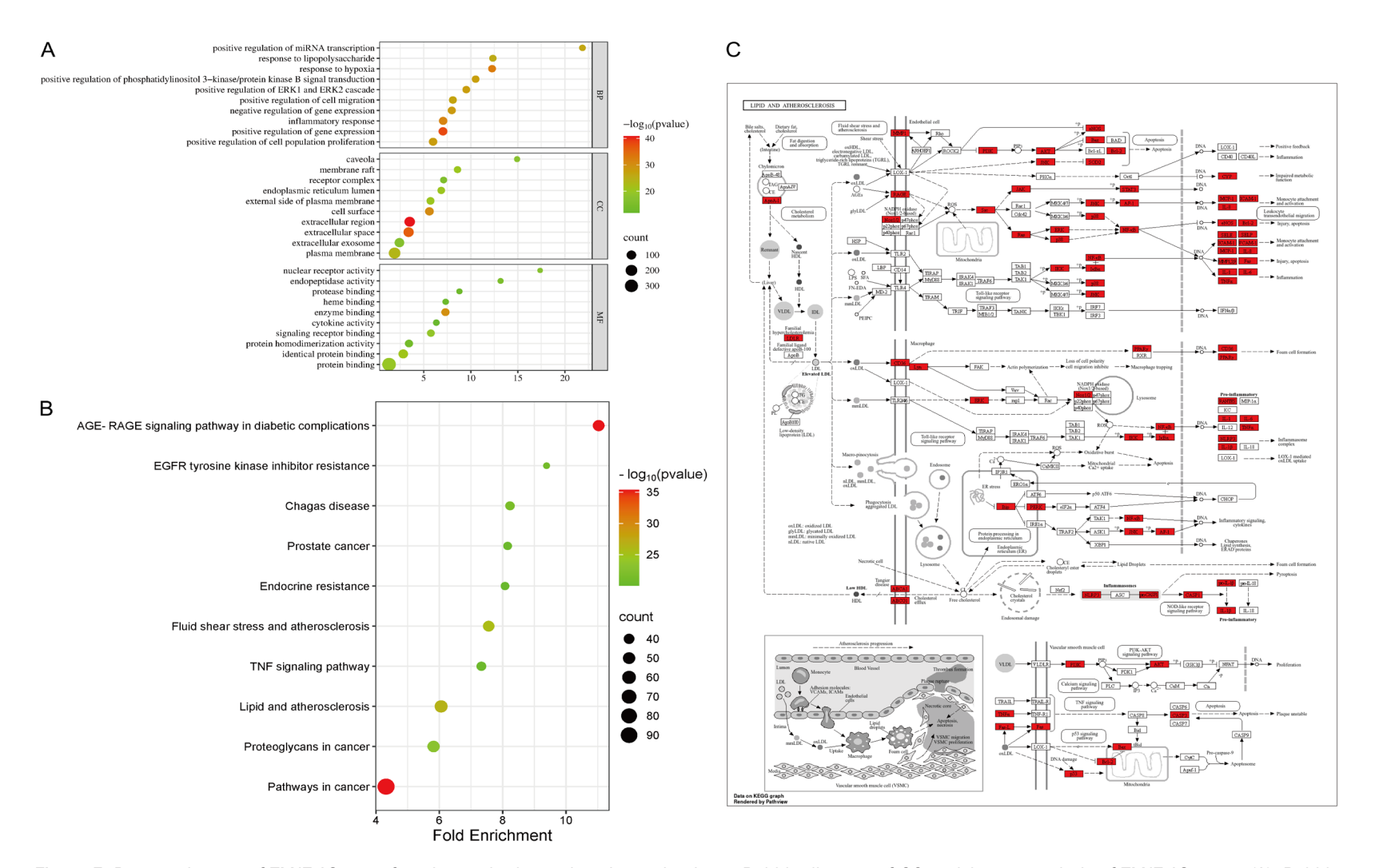


Figure 5. Panoramic map of TMJZ-AS gene function and atherosclerosis mechanisms. Bubble diagram of GO enrichment analysis of TMJZ-AS genes (A). Bubble diagram of the KEGG enrichment pathway of TMJZ-atherosclerosis genes (B). Map of lipid and atherosclerosis (C). TMJZ, Tongmai Jiangzuo Decoction; AS, Atherosclerosis; GO, Gene Ontology; KEGG, Kyoto Encyclopedia of Genes and Genomes.

Table 3. Molecular docking analysis

Mol ID	Molecule Name	Target	PDB ID	Binding ability (kcal/mol)
MOL002714	Baicalein	CD36	5LGD	-8.0
MOL001406	Crocetin	CD36	5LGD	-10.2
MOL011156	Epoxyganoderiol-A	CD36	5LGD	-8.3
MOL011256	Ganolucidic-Acid-E	CD36	5LGD	-9.0
MOL002714	Baicalein	PPARγ	1ZGY	-8.2
MOL001406	Crocetin	PPARγ	1ZGY	-6.9
MOL011156	Epoxyganoderiol-A	PPARγ	1ZGY	-7.3
MOL011256	Ganolucidic-Acid-E	PPARγ	1ZGY	-7.6

PDB, Protein Data Bank; CD36, CD36 molecule; PPARy, peroxisome proliferator activated receptor gamma.

1183 target genes; two active ingredients of *Chuanxiong Rhizoma*, corresponding to 200 target genes; 8 active components of red *peony roots*, corresponding to 230 target genes; 6 active ingredients of *Leonurus leonurus*, corresponding to 271 target genes; 13 active ingredients of the *leech*, corresponding to 342 target genes; 4 active ingredients of *Rhizoma alismatis*, corresponding to 198 target genes; 7 active components of *Cassia seeds*, corresponding to 178 target genes; and 9 active components in *lotus leaves*, corresponding to 256 target genes. After duplication removal, a total of 2039 genes were obtained.

Target genes of TMJZ in AS

The GeneCards and OMIM databases contain 979 and 550 genes related to "atherosclerosis" and "coronary heart disease", respectively. After removing duplicate values, 1493 AS-related genes were obtained. By intersecting these with the target gene data of TMJZ, 395 target genes of TMJZ associated with AS were identified (Figure 2).

CDT network construction and topological network analysis

To further investigate compounds and potential targets, CDT networks with 662 nodes and 4749 edges were created using Cytoscape (Figure 3). The turmeric V nodes represent fifteen botanical drugs from the TMJZ. The green circular nodes represent the compounds of each botanical drug. Circular purple nodes represent AS target genes. The larger the nodes, the higher the degrees. The top compounds and genes were selected according to their size

and degree values, as shown in **Tables 1** and **2**, respectively.

PPI network construction and analysis

After setting "Homo sapiens" as the species and a minimum required interaction score of 0.90, the PPI network (Figure 4A) contained 336 nodes (protein names) and 2642 edges (interactions). Cytoscape 3.8.2 was used to generate core networks with the follow-

ing criteria: BC > 200.95, Closeness centrality (CC) > 0.27, DC > 10 (**Figure 4B**). Central analysis and evaluation were performed using CytoNCA.

After the first screening, 106 nodes and 1210 edges were identified (**Figure 4C**). With the criteria set to BC > 69.03, Closeness centrality (CC) > 0.42, DC > 20, a second screening yielded 20 nodes and 178 edges (**Figure 4D**).

GO and KEGG pathway enrichment analysis

BP, cellular components (CC), and MF were included in the GO analysis. Bioinformatic analvsis revealed that the main enriched BPs associated with TMJZ intervention in AS included positive regulation of gene expression, response to hypoxia, inflammatory response, negative regulation of gene expression, positive regulation of cell population proliferation, positive regulation of the ERK1 and ERK2 cascades, positive regulation of phosphatidylinositol 3-kinase/protein kinase B signal transduction, positive regulation of cell migration, positive regulation of miRNA transcription, and response to lipopolysaccharide. The enriched CCs included extracellular region, extracellular space, cell surface, plasma membrane, ER lumen, membrane raft, caveolar, extracellular exosome, and receptor complex. The enriched MFs included enzyme binding, identical protein binding, protein binding, signaling receptor binding, nuclear receptor activity, endopeptidase activity, protein homodimerization activity, protease binding, heme binding, and cytokine activity (Figure 5A). TMJZ is primarily involved in lipid and atherosclerosis, fluid shear stress and atherosclerosis, endocrine resistance, and the TNF pathway (Figure 5B, 5C).

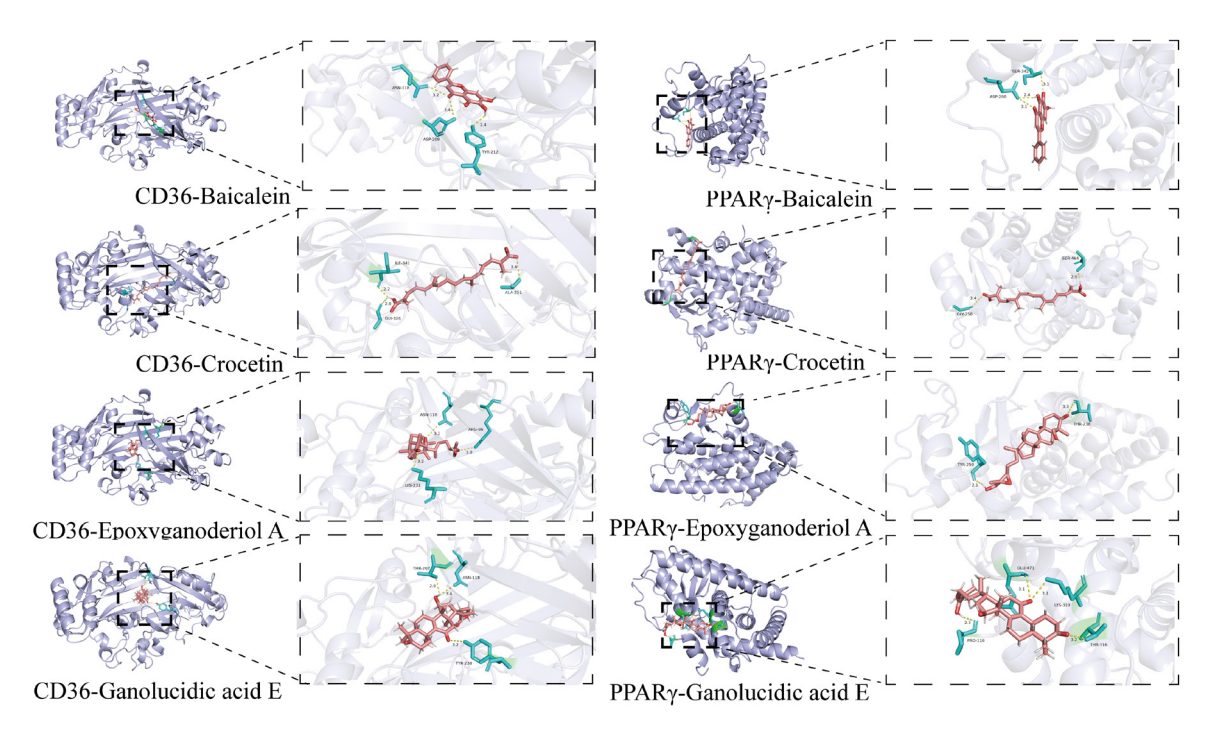


Figure 6. Results of molecular docking. CD36, CD36 molecule; PPARγ, peroxisome proliferator activated receptor gamma.

Molecular docking analysis

Four key components (crocetin, epoxyganoderiol A, baicalein, and ganolucidic acid E) were chosen for molecular docking with PPARγ and CD36 (Table 3 and Figure 6). According to the docking results, lower binding energy values indicate stronger binding affinity. All the components presented binding energies below -5 kcal/mol, reflecting strong interactions with the target proteins. The most stable complexes were crocetin (MOLO01406) and CD36 (binding energy: -10.2 kcal/mol). Visualization of this stable complex via PyMOL (Figure 6) revealed the specific binding sites on the protein amino acid chains and hydrogen-bond interactions.

Effects of TMJZ on body weight and blood lipid levels of mice

After modeling according to the experimental scheme shown in figure (Figure 7A), the weight of all groups increased with time. Mice in the TMJZ and Model groups gained more rapid body weight (Figure 7B). After 12 weeks of treatment, TMJZ significantly reduced body weight compared to the Model group (Figure 7C). Serum TG, TC, LDL-C, and ox-LDL levels were significantly increased after AS model establishment, which was drastically decreased by 12-week TMJZ and ARA supplement (P <

0.01) (**Figure 7G**, **7H**). However, HDL-C level was decreased in the Model group and was not affected by TMJZ (**Figure 7D-F**).

Effects of TMJZ on inflammatory factors

AS significantly elevated serum levels of TNF- α , IL-6 and IL-1 β (P < 0.01), which were sharply decreased by ARA and TMJZ (P < 0.01). For TNF- α level, ARA demonstrated a more notable decrease compared to TMJZ group (P < 0.05); while for IL-6 and IL-1 β reduction, ARA and TMJZ groups demonstrated comparable effects (P < 0.05, **Table 4**).

TMJZ attenuated atherosclerosis in ApoE-/mice

H&E staining revealed that AS sharply increased plaque areas, which were drastically decreased by TMJZ and ARA (P < 0.01) (Figure 8A, 8B). Oil red O staining of the aortic arch revealed no lipid plaques in the controls but rather large lipid plaques in the AS mice, which were sharply decreased by the TMJZ in the ApoE-/- mice (Figure 8C).

TMJZ suppressed CD36 but enhanced PPARy

Immunohistochemical staining revealed that AS significantly upregulated CD36 but down-

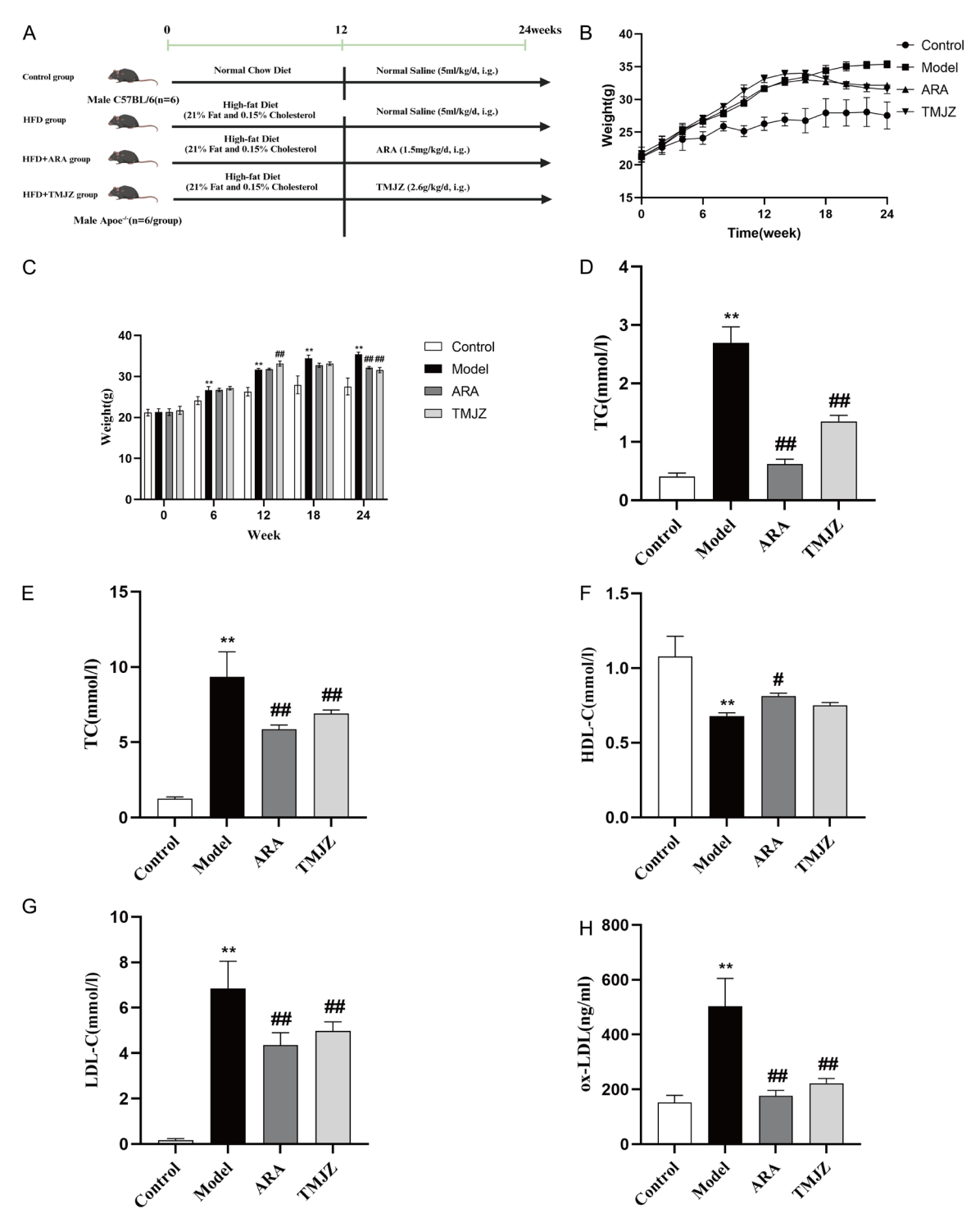


Figure 7. TMJZ reduced lipid levels in ApoE-/- mice. (A) A schematic of the experimental protocol, (B) Line plot of body weight, (C) Body weight of mice in each time period, (D) serum total cholesterol (TG) level, (E) serum triglyceride (TC) level, (F) serum high-density lipoprotein cholesterol (HDL-C) level, (G) serum low-density lipoprotein cholesterol (LDL-C) level, and (H) Serum oxidized low-density lipoprotein (ox-LDL) level. **P < 0.01 vs. Control group, ##P < 0.01 vs. Model group.

regulated PPAR γ (P < 0.01), which was reversed by intervention with the TMJZ and ARA (P <

0.05, P < 0.01) (**Figure 9**). These results were also confirmed by western blot (**Figure 10**).

Table 4. Comparison of inflammatory cytokines among groups

Group	n	TNF-α (ng/L)	IL-6 (ng/L)	IL-1β (ng/L)
Control	6	87.65±26.14	59.64±5.65	16.85±2.31
Model	6	195.86±24.35°	96.35±6.32°	35.64±2.47a
ARA	6	147.74±32.14 ^{a,b}	71.54±5.79 ^{a,b}	23.67±2.12 ^{a,b}
TMJZ	6	156.78±28.65 ^{a,b,e}	76.85±6.87 ^{a,b}	26.54±2.76a,b

 $^{\rm e}P$ < 0.01, compared with the control group; $^{\rm b}P$ < 0.01, compared with the model group; $^{\rm e}P$ < 0.05, compared with the ARA group. TNF-α, tumor necrosis factor-alpha; IL-6, interleukin-6; IL-1β, interleukin-1 beta; ARA, atorvastatin; TMJZ, Tongmai Jiangzhuo Decoction.

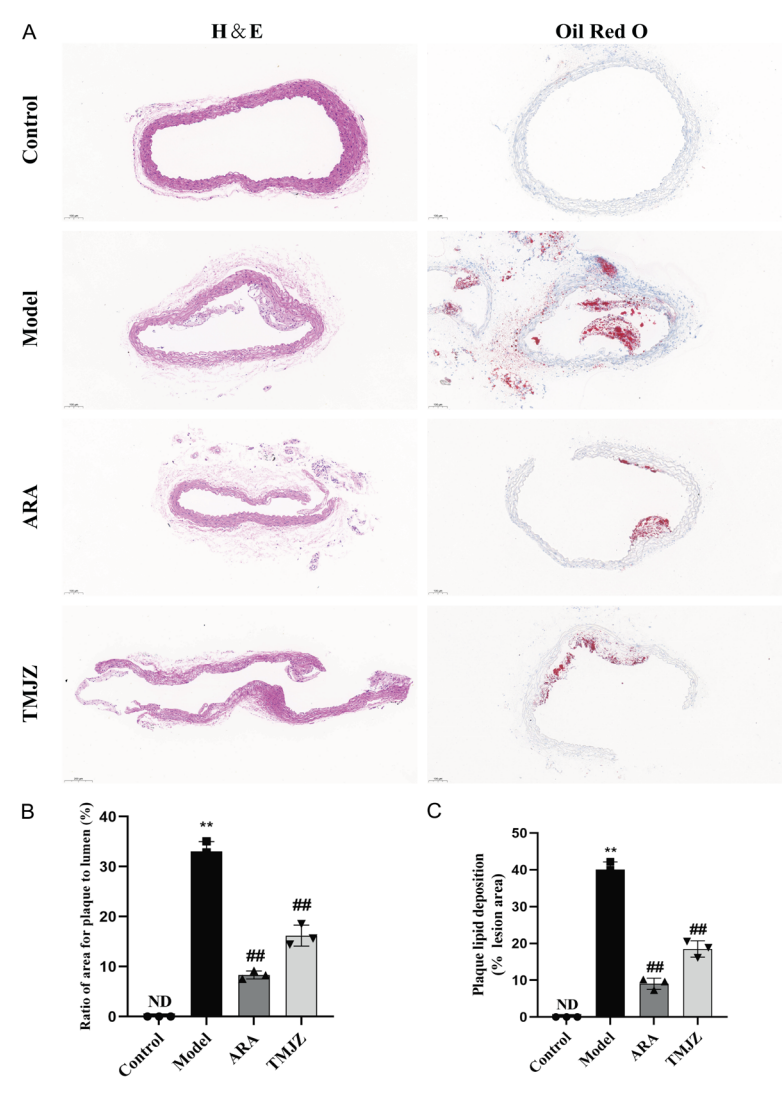


Figure 8. TMJZ ameliorated atherosclerotic lesions in ApoE-/- mice. A. H&E staining and Oil Red staining showed that TMJZ effectively reduced the aortic plaque area in AS mice. B. Quantitative analysis of plaque area. C. Quantitative analysis of lipid deposition. **P < 0.01 vs Control group, ##P < 0.01 vs Model group; N = 3 per group. TMJZ, Tongmai Jiangzuo Decoction; AS, Atherosclerosis; HE, Hematoxylin and eosin; Oil Red O, Oil Red O stain (lipophilic dye).

These results suggest that the TMJZ may regulate lipid metabolism and improve AS by regu-

lating the PPARy/CD36 signaling pathway.

TMJZ enhanced ABCA1 and LXRα

Immunoblotting (Figure 10) revealed that AS drastically decreased LXR α and ABCA1, which were reversed by TMJZ and ARA (P < 0.01). These findings suggest that the TMJZ may suppress atherosclerosis development by upregulating LXR α /ABCA1 to increase cholesterol transport and maintain intracellular cholesterol homeostasis, reducing foam cell formation.

Discussion

Current studies suggest that AS is a chronic inflammatory disease of the arterial intima, characterized by imbalance of lipid homeostasis [15]. Therefore, maintaining optimal lipid levels in the body is crucial to achieve ideal cardiovascular health [16]. TMJZ shows significant potential in this regard.

As the main active ingredients of Ganoderma lucidum, Ganoderma lucidum polysaccharides (GLP) suppresses inflammation and ROS, affects gut microbiota, improves blood glucose and lipid levels, and help control obesity [17]. Active components of Astragali Radix (AR), mainly triterpene saponins, flavonoid, and polysaccharides, are well-studied and has been shown to regulate a variety of diseases including AS [18]. Panax notoginseng saponins (PNSs), as the major active component of P. notoginseng, suppress AS progression in ApoE-/- mice by inhibiting mo-

nocyte chemoattractant protein-1 (MCP-1) [19]. In addition, PNSs improve lipid metabolism and

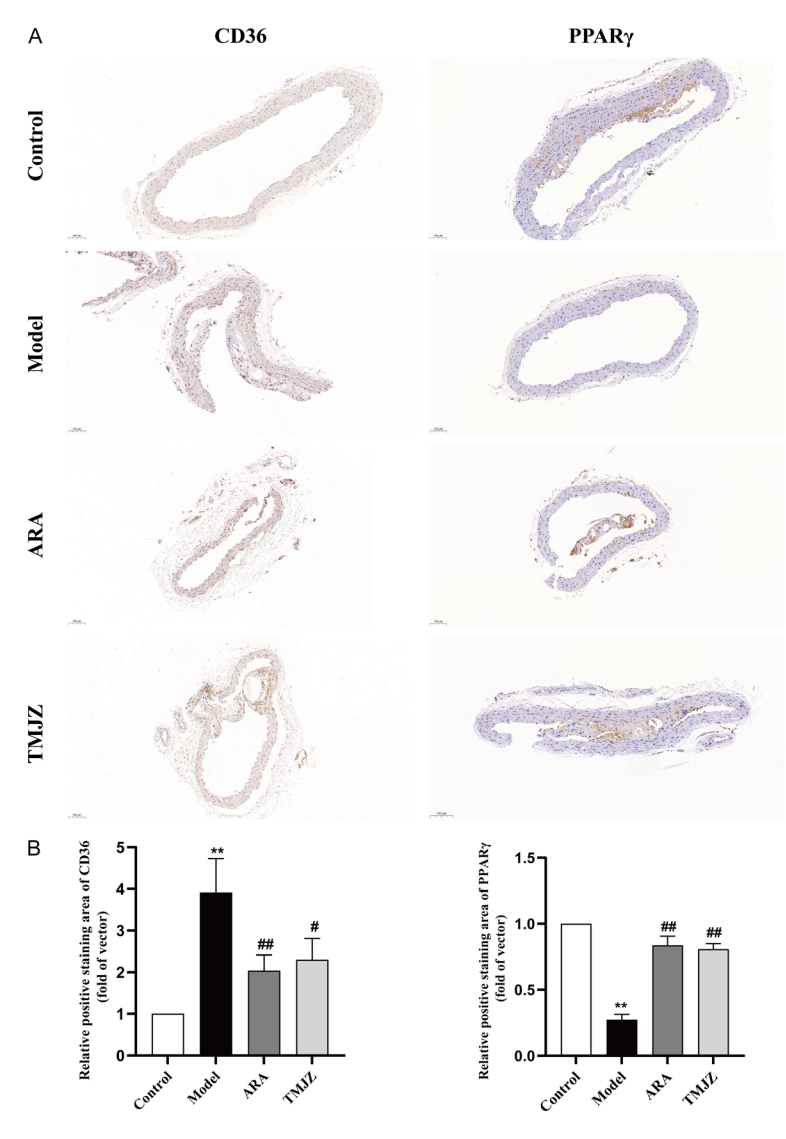


Figure 9. Effect of TMJZ on the expression of CD36 and PPAR γ in the aortic arch. A. Representative pictures of CD36 and PPAR γ immunohistochemical staining in the aortic arch of each group. B. The area of positive staining was measured using the image J analysis software and homogenized. **P < 0.01 vs Control group, #P < 0.05 vs Model group, ##P < 0.01 vs Model group; N = 6 per group. TMJZ, Tongmai Jiangzuo Decoction; CD36, CD36 molecule; PPAR γ , peroxisome proliferator activated receptor gamma.

attenuate AS through suppressing phosphory-lated focal adhesion kinase (p-FAK) and nuclear factor kappa B (NF-kB) translocation [20]. In this study, a high-fat diet significantly up-regulated serum levels of TC, TG and LDL-C and down-regulated HDL-C in APOE-/- mice, resulting in the typical "porridge" -like lesions in the arterial intima of the mice, with obvious accumulation of lipid in the plaque. The application of TMJZ effectively reversed this outcome. These findings suggest that the lipid-lowering effects of TMJZ were similar to that of atorvastatin, further validating the prominent role of

TMJZ in the treatment of diseases caused by dyslipidemia.

PPARy is a transcription factor activated by fatty acid metabolism ligands. It regulates its own gene transcription after interacting with target factors, exerting various biochemical effects, including the regulation of cell proliferation, differentiation, and the inflammatory response, especially in macrophage lipid metabolism [21]. CD36, a member of the scavenger receptor type B family, is a key component of foam cell formation and a major pro-atherosclerotic factor due to its ability to mediate the uptake of ox-LDL by macrophages [22]. On the one hand, the combination of CD36 and ox-LDL activates the protein kinase signaling pathway, aggravates the subintimal deposition of lipids, and promotes AS lesions [23]. On the other hand, CD36mediated endocytosis of ox-LDL on macrophages also activates PPARy, accelerating the reverse transport of excess cholesterol in foam cells, thus promoting cholesterol efflux and exerting an anti-AS effect [24]. Under normal physiological conditions, CD36mediated lipid uptake and efflux, triggered by activated PPARy, are normally in a dynamic balance. Under patho-

logical conditions, the activity of cholesteryl ester transfer protein (CETP) is inhibited, leading to lipid transport disorders and increased cholesterol accumulation in macrophages. Excess free cholesterol is re-esterified to form cholesteryl ester under the action of the endoplasmic reticulum-resident protein ACAT1 and accumulates in lipid droplets, thereby promoting the gradual transformation of macrophages into foam cells [25]. IHC staining revealed that the TMJZ could increase PPARy and suppress CD36 in aortic tissues, indicating that the TMJZ has a targeted regulatory effect on the PPARy/

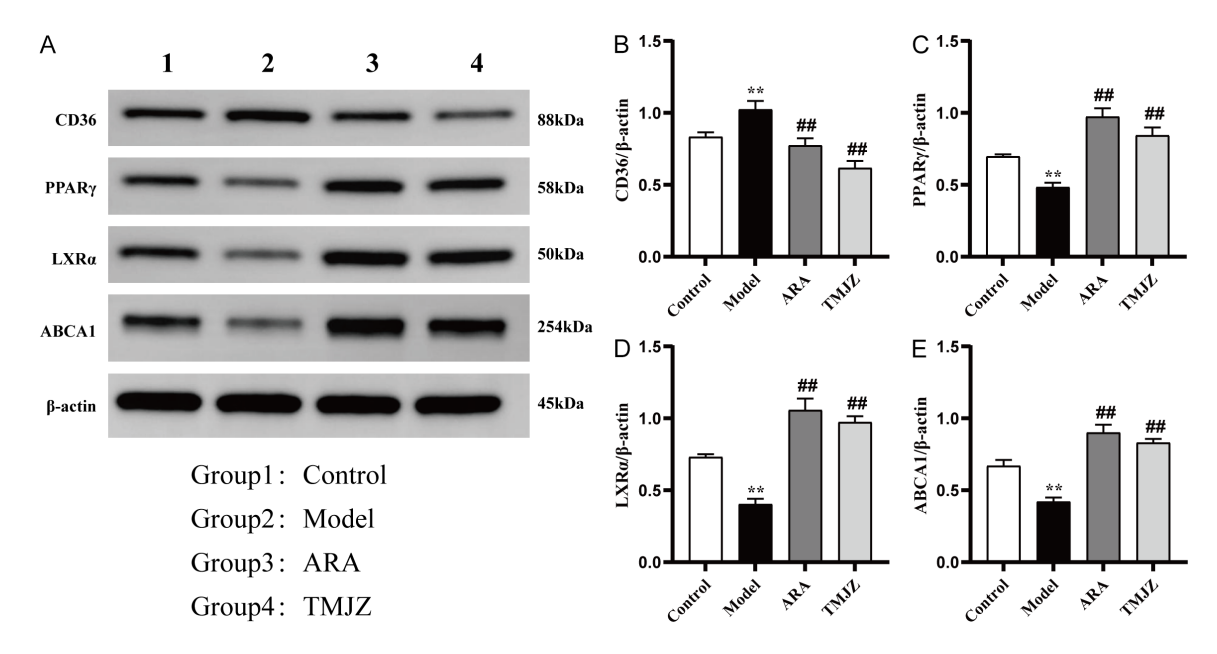


Figure 10. Effects of TMJZ on aortic lipid-phagocytic and reverse cholesterol transport-related proteins in atherosclerosis. A. Representative western blot Images of CD36, PPARγ, LXR α , and ABCA1 in the Aorta of Each Group. B-E. Measurement of the Electrophoretic B and Area of Target Proteins Using Image J Software and Calculation of the Ratio of Target Protein Area to β -actin Area. **P < 0.01 vs. Control group, ##P < 0.01 vs. Model group; N = 6 per group.

CD36 signaling pathway, which may participate in the lipid metabolism of macrophages, maintain the balance between lipid uptake and efflux and prevent subsequent lesions caused by foam cell generation.

Conclusion

TMJZ can effectively protect the arterial intimal structure, improve lipid metabolism, and delay AS progression, likely by regulating the PPARy/CD36 pathway to stimulate cholesterol efflux in macrophages, suppress the uptake of oxidized modified lipids, and reduce foam cell formation.

Acknowledgements

We are grateful to the Yunnan Research Center for Traditional Chinese Medicine and Preventive Medicine for providing laboratory space and experimental guidance. This work was supported by Special Foundation of Yunnan Fundamental Research of Traditional Chinese Medicine (grant No. 202101AZ070001-274).

Disclosure of conflict of interest

None.

Address correspondence to: Jie Xia, The First Affiliated Hospital of Yunnan University of Chinese

Medicine, Kunming 650021, Yunnan, China. E-mail: jie_X1365@163.com; Guihui Wang, The Third Affiliated Hospital of Yunnan University of Chinese Medicine, Kunming 650000, Yunnan, China. E-mail: Wgh_1234566@163.com

References

- Libby P. The changing landscape of atherosclerosis. Nature 2021; 592: 524-533.
- [2] Luca AC, David SG, David AG, Țarcă V, Pădureț IA, Mîndru DE, Roşu ST, Roşu EV, Adumitrăchioaiei H, Bernic J, Cojocaru E and Țarcă E. Atherosclerosis from newborn to adult-epidemiology, pathological aspects, and risk factors. Life (Basel) 2023; 13: 2056.
- [3] Mensah GA, Fuster V, Murray CJL and Roth GA; Global Burden of Cardiovascular Diseases and Risks Collaborators. Global burden of cardiovascular diseases and risks, 1990-2022. J Am Coll Cardiol 2023; 82: 2350-2473.
- [4] Andreou I, Stone PH, Ikonomidis I, Alexopoulos D and Sabaté M. Recurrent atherosclerosis complications as a mechanism for stent failure. Hellenic J Cardiol 2020; 61: 9-14.
- [5] Kouhpeikar H, Delbari Z, Sathyapalan T, Simental-Mendía LE, Jamialahmadi T and Sahebkar A. The effect of statins through mast cells in the pathophysiology of atherosclerosis: a review. Curr Atheroscler Rep 2020; 22: 19.
- [6] Wu M, Li X, Wang S, Yang S, Zhao R, Xing Y and Liu L. Polydatin for treating atherosclerotic dis-

- eases: a functional and mechanistic overview. Biomed Pharmacother 2020; 128: 110308.
- [7] Zhao L, Zhang H, Li N, Chen J, Xu H, Wang Y and Liang Q. Network pharmacology, a promising approach to reveal the pharmacology mechanism of Chinese medicine formula. J Ethnopharmacol 2023; 309: 116306.
- [8] Luo TT, Lu Y, Yan SK, Xiao X, Rong XL and Guo J. Network pharmacology in research of Chinese Medicine Formula: methodology, application and prospective. Chin J Integr Med 2020; 26: 72-80.
- [9] Wang Y, Liu M, Jafari M and Tang J. A critical assessment of Traditional Chinese Medicine databases as a source for drug discovery. Front Pharmacol 2024; 15: 1303693.
- [10] Liu Z, Guo F, Wang Y, Li C, Zhang X, Li H, Diao L, Gu J, Wang W, Li D and He F. BATMAN-TCM: a bioinformatics analysis tool for molecular mechANism of Traditional Chinese Medicine. Sci Rep 2016; 6: 21146.
- [11] Sherman BT, Hao M, Qiu J, Jiao X, Baseler MW, Lane HC, Imamichi T and Chang W. DAVID: a web server for functional enrichment analysis and functional annotation of gene lists (2021 update). Nucleic Acids Res 2022; 50: W216-W221.
- [12] The Gene Ontology Consortium. Expansion of the Gene Ontology knowledgebase and resources. Nucleic Acids Res 2017; 45: D331-D338.
- [13] Reagan-Shaw S, Nihal M and Ahmad N. Dose translation from animal to human studies revisited. FASEB J 2008; 22: 659-661.
- [14] Gu Y, Jiang J, Zhang Y, Chen Y, Chen Y, Jiang W, Huang Z and Zhou F. Congxin Lunzhi Fang improves aortic atherosclerosis and regulates ACE2 expression in ApoE-/- mice. Nan Fang Yi Ke Da Xue Xue Bao 2021; 41: 1623-1630.
- [15] Soehnlein O and Libby P. Targeting inflammation in atherosclerosis from experimental insights to the clinic. Nat Rev Drug Discov 2021; 20: 589-610.
- [16] Dong J, Yang S, Zhuang Q, Sun J, Wei P, Zhao X, Chen Y, Chen X, Li M, Wei L, Chen C, Fan Y and Shen C. The associations of lipid profiles with cardiovascular diseases and death in a 10year prospective cohort study. Front Cardiovasc Med 2021; 8: 745539.

- [17] Ma Y, Han J, Wang K, Han H, Hu Y, Li H, Wu S and Zhang L. Research progress of Ganoderma lucidum polysaccharide in prevention and treatment of Atherosclerosis. Heliyon 2024; 10: e33307.
- [18] Li M, Han B, Zhao H, Xu C, Xu D, Sieniawska E, Lin X and Kai G. Biological active ingredients of Astragali Radix and its mechanisms in treating cardiovascular and cerebrovascular diseases. Phytomedicine 2022; 98: 153918.
- [19] Liu C, Feng R, Zou J, Xia F and Wan JB. 20(S)-Protopanaxadiol Saponins Mainly Contribute to the anti-atherogenic effects of panax notoginseng in ApoE deficient mice. Molecules 2019; 24: 3723.
- [20] Duan L, Xiong X, Hu J, Liu Y, Li J and Wang J. Panax notoginseng saponins for treating coronary artery disease: a functional and mechanistic overview. Front Pharmacol 2017; 8: 702.
- [21] Zuo S, Wang Y, Bao H, Zhang Z, Yang N, Jia M, Zhang Q, Jian A, Ji R, Zhang L, Lu Y, Huang Y and Shen P. Lipid synthesis, triggered by PPARy T166 dephosphorylation, sustains reparative function of macrophages during tissue repair. Nat Commun 2024; 15: 7269.
- [22] Shu H, Peng Y, Hang W, Nie J, Zhou N and Wang DW. The role of CD36 in cardiovascular disease. Cardiovasc Res 2022; 118: 115-129.
- [23] Tian K, Xu Y, Sahebkar A and Xu S. CD36 in atherosclerosis: pathophysiological mechanisms and therapeutic implications. Curr Atheroscler Rep 2020; 22: 59.
- [24] Chen Y, Zhang J, Cui W and Silverstein RL. CD36, a signaling receptor and fatty acid transporter that regulates immune cell metabolism and fate. J Exp Med 2022; 219: e20211314.
- [25] Lee-Rueckert M, Lappalainen J, Leinonen H, Plihtari R, Nordström T, Åkerman K, Öörni K and Kovanen PT. Acidic extracellular pH promotes accumulation of free cholesterol in human monocyte-derived macrophages via inhibition of ACAT1 activity. Atherosclerosis 2020; 312: 1-7.